pISSN 1598-2998, eISSN 2005-9256

https://doi.org/10.4143/crt.2020.1221

Cancer Res Treat. 2022;54(1):234-244

Original Article

Prediction of Pathologic Findings with MRI-Based Clinical Staging Using the Bayesian Network Modeling in Prostate Cancer: A Radiation Oncologist Perspective

Chan Woo Wee[1,2], **Bum-Sup Jang**[3], **Jin Ho Kim**[2,4,5], **Chang Wook Jeong**[6], **Cheol Kwak**[6], **Hyun Hoe Kim**[6], **Ja Hyeon Ku**[6], **Seung Hyup Kim**[7], **Jeong Yeon Cho**[7], **Sang Youn Kim**[7]

[1]Department of Radiation Oncology, SMG-SNU Boramae Medical Center, Seoul, [2]Department of Radiation Oncology, Seoul National University College of Medicine, Seoul, [3]Department of Radiation Oncology, Seoul National University Bundang Hospital, Seongnam, [4]Cancer Research Institute, Seoul National University College of Medicine, Seoul, [5]Institute of Radiation Medicine, Seoul National University College of Medicine, Seoul, Departments of [6]Urology and [7]Radiology, Seoul National University College of Medicine, Seoul, Korea

Purpose This study aimed to develop a model for predicting pathologic extracapsular extension (ECE) and seminal vesicle invasion (SVI) while integrating magnetic resonance imaging-based T-staging (cT_{MRI}, cT1c-cT3b).

Materials and Methods A total of 1,915 who underwent radical prostatectomy between 2006-2016 met the inclusion/exclusion criteria. We performed a multivariate logistic regression analysis as well as Bayesian network (BN) modeling based on possible confounding factors. The BN model was internally validated using 5-fold validation.

Results According to the multivariate logistic regression analysis, initial prostate-specific antigen (iPSA) (β=0.050, p < 0.001), percentage of positive biopsy cores (PPC) (β=0.033, p < 0.001), both lobe involvement on biopsy (β=0.359, p=0.009), Gleason score (β=0.358, p < 0.001), and cT_{MRI} (β=0.259, p < 0.001) were significant factors for ECE. For SVI, iPSA (β=0.037, p < 0.001), PPC (β=0.024, p < 0.001), Gleason score (β=0.753, p < 0.001), and cT_{MRI} (β=0.507, p < 0.001) showed statistical significance. BN models to predict ECE and SVI were also successfully established. The overall area under the receiver operating characteristic curve (AUC)/accuracy of the BN models were 0.76/73.0% and 0.88/89.6% for ECE and SVI, respectively. According to internal comparison between the BN model and Roach formula, BN model had improved AUC values for predicting ECE (0.76 vs. 0.74, p=0.060) and SVI (0.88 vs. 0.84, p < 0.001).

Conclusion Two models to predict pathologic ECE and SVI integrating cT_{MRI} were established and installed on a separate website for public access to guide radiation oncologists.

Key words Prostate neoplasms, Radiotherapy, Magnetic resonance imaging, Bayesian network, Extracapsular extension, Seminal vesicle

Introduction

Adenocarcinoma of the prostate (PCa) is the most common cancer among males from the Unites States, with over 170,000 estimated new cases in 2019 [1]. Although not as frequently diagnosed as in western countries, the incidence of PCa is also rapidly rising in Korea [2]. For localized PCa patients who are not candidates for active surveillance, primary radiotherapy (RT) with or without androgen deprivation therapy is one of the standard treatment modalities throughout all risk groups [3,4].

In external beam RT for PCa, accurate target volume delineation is crucial due to the routine use of intensity-modulated RT and the increasing utilization of hypofractionated RT, including stereotactic body RT [5]. For intermediate-to-high risk localized PCa, extra-margins to cover potential extracapsular extension (ECE) should be considered, as well as the inclusion of the seminal vesicles (SVs) in the target volume [6]. Therefore, precise prediction of the risk of ECE or seminal vesical invasion (SVI) is of importance for patients without clinically overt ECE and SVI, since larger RT-target volumes would result in unnecessary excess radiation exposure to the bladder and rectum. For example, based on pathological findings, the European Organisation for Research and Treatment of Cancer (EORTC) recommends the clinical target volumes to include at least the proximal 1.4 cm and 2.2 cm of the SV for intermediate- and high-risk patients, respectively [6]. The current Radiation Therapy Oncology Group

Correspondence: Jin Ho Kim
Department of Radiation Oncology, Cancer Research Institute, Institute of Radiation Medicine, Seoul National University College of Medicine, 101 Daehak-ro, Jongno-gu, Seoul 03080, Korea
Tel: 82-2-2072-4767 Fax: 82-2-765-3317 E-mail: jinho.kim.md@gmail.com
Received November 19, 2020 **Accepted** May 16, 2021 **Published Online** May 17, 2021
*Chan Woo Wee and Bum-Sup Jang contributed equally to this work.

(RTOG) protocols include the proximal 1.0-2.0 cm portion for intermediate- to high-risk patients. These recommendations are convenient and simple for radiation oncologists to adopt. However, further individualization based on risk factors might be necessary because discrepancies between clinical and pathologic stages exist, even in low-risk PCa [7].

The current National Comprehensive Cancer Network (NCCN) risk grouping for PCa is mainly based on clinical staging, initial prostate-specific antigen (iPSA), and Gleason score (GS) obtained from biopsy [4]. Of these, the clinical T-stage should be determined only by the findings of a digital rectal exam. Referring to findings from magnetic resonance imaging (MRI) or tumor laterality from biopsy specimens is discouraged in the 8th American Joint Committee on Cancer (AJCC) staging system [8]. However, the yield of predicting ECE or SVI by digital rectal exam alone is low. Furthermore, it has been reported that the addition of preoperative MRI increases the accuracy of predicting whether the disease is pathologically organ-confined or not [9-11].

The Bayesian network (BN) model is a statistical framework that represents the conditional dependencies of variables via a directed acyclic graph (DAG). In DAG, nodes indicate clinical variables and edges demonstrate conditional dependencies. The strength of BN is accommodating the heterogeneity between clinical or non-clinical variables and providing interpretable clinical scenarios or probabilities to clinicians. Previous studies have facilitated the use of BN for the prediction of prognosis various in cancers, such as breast cancer and gallbladder cancer [12,13]. BN can mimic the human decision-making process, which reveals the surgical indication for patients with gallbladder cancer [14].

Thus, in the current study, we sought BN modeling to predict pathologic findings, such as ECE and SVI in patients with PCa. Specifically, in order to guide radiation oncologists for further individualized target contouring based on MRI findings, we established BN models to accurately predict the risk of pathological ECE and SVI by integrating the MRI findings into clinical T-staging. Furthermore, the positivity rate of the resection margin (RM+ve) was also predicted since these patients are future candidates for salvage RT with increased risk of biochemical relapse [3,4]. This information would be useful not only for radiation oncologists, but for urologists planning surgery.

Materials and Methods

1. Patients and imaging

Patients with PCa confirmed by transrectal ultrasound-guided biopsy and who are undergoing preoperative MRI with radical prostatectomy between 2006 and 2016 were included in the study. All patients were required to have at least eight or more biopsy cores obtained at diagnosis. To minimize patient heterogeneity, those who met the following criteria were excluded: (1) incidentally diagnosed PCa by transurethral prostatectomy for benign prostatic hyperplasia, (2) clinically overt T4 or N1 disease on preoperative imaging, (3) non-adenocarcinoma PCa, (4) history of any anti-PCa treatment such as neoadjuvant androgen deprivation therapy prior to radical prostatectomy, and (5) no information regarding iPSA or MRI within 6 months preoperately. A total of 1915 patients met the inclusion and exclusion criteria. Patient characteristics are shown in

Table 1. Patient and tumor characteristics

Variable	No. (%)
Total	1,915 (100)
Age, median (range, yr)	67 (41-86)
iPSA (ng/mL)	
Below 4	190 (9.9)
4-10	1,126 (58.8)
10-20	387 (20.2)
20 or higher	212 (11.1)
TRUS-Bx	
PPC, median (range, %)	25.0 (5.0-100.0)
Both lobe involvement	
Yes	797 (41.6)
No	1,076 (56.2)
Unknown	42 (2.2)
Gleason score	
6	863 (45.1)
7(3+4)	389 (20.3)
7(4+3)	297 (15.5)
8	277 (14.5)
9	78 (4.1)
10	11 (0.6)
cT_{MRI} stage[a]	
1c	243 (12.7)
2a-2b	718 (37.5)
2c	694 (36.2)
3a	110 (5.7)
3b	150 (7.8)
Pathologic findings[b]	
ECE	702 (36.7)
SVI	227 (11.9)
RM+ve	719 (37.5)

cT_{MRI}, magnetic resonance imaging–based T-staging; ECE, extracapsular extension, iPSA, initial prostate-specific antigen; PPC, percentage of positive biopsy cores; RM+ve, positive resection margin; SVI, seminal vesicle invasion; TRUS-Bx, transrectal ultrasound-guided biopsy. [a]Clinical stage according to magnetic resonance imaging findings, [b]Radical prostatectomy specimen.

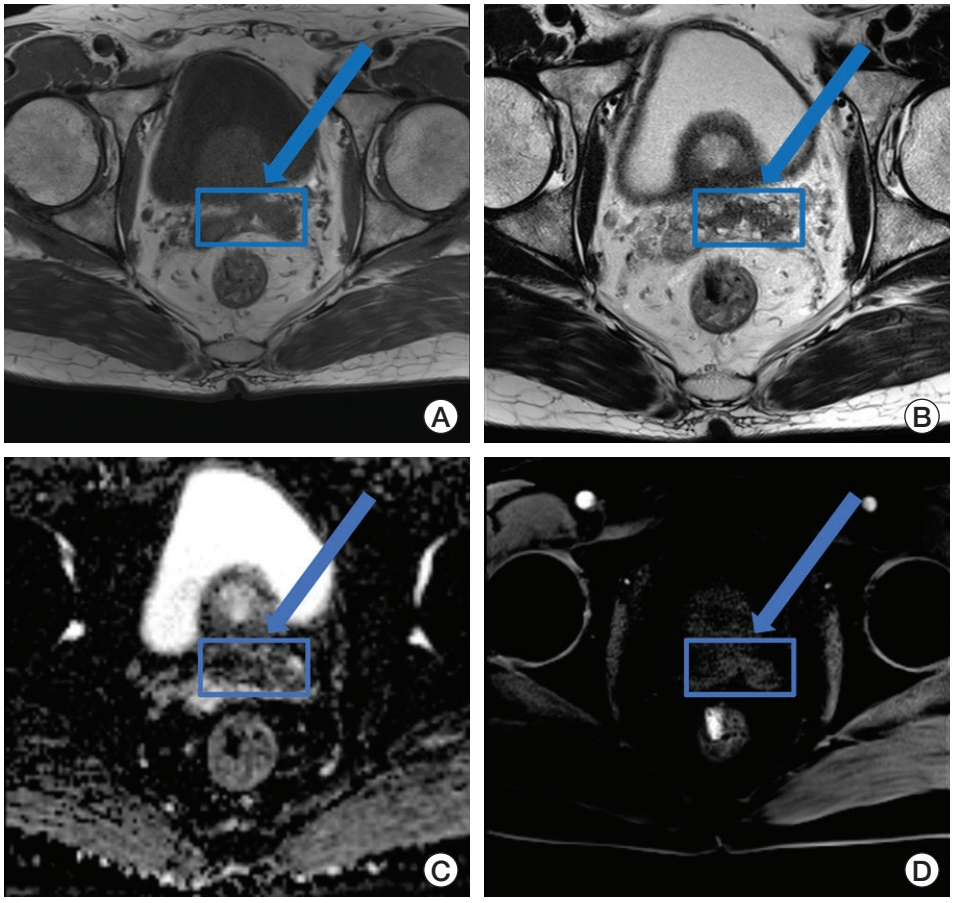

Fig. 1. A preoperative multiparametric 3.0T magnetic resonance imaging using T1-weighted (A), T2-weighted (B), diffusion-weighted (C), and dynamic contrast-enhanced (D) images in a 67-year-old male diagnosed as prostate cancer by biopsy. Lesion with suspected seminal vesicle invasion (cT_{MRI}3b) shows low signal intensity on T2- (B) and diffusion-weighted (C) images with contrast enhancement (D).

Table 2. Results of multivariate logistic regression analysis

Variable	ECE		SVI		RM+ve	
	β	p-value	β	p-value	β	p-value
iPSA (ng/mL)	0.050	< 0.001	0.037	< 0.001	0.038	< 0.001
PPC (%)	0.033	< 0.001	0.024	< 0.001	0.021	< 0.001
BLI-Bx	0.359	0.009	–0.003	0.988	–0.177	0.161
Gleason scores on biopsy	0.358	< 0.001	0.753	< 0.001	0.131	0.037
cT_{MRI} stage[a)]	0.259	< 0.001	0.507	< 0.001	0.149	0.006
Constant	–5.486	< 0.001	–10.459	< 0.001	–2.894	< 0.001

cT_{MRI}, magnetic resonance imaging–based T-staging; BLI-Bx, both lobe involvement on biopsy; ECE, extracapsular extension; iPSA, initial prostate-specific antigen; PPC, percentage of positive biopsy cores; RM+ve, positive resection margin; SVI, seminal vesicle invasion.
[a)]Clinical stage according to magnetic resonance imaging findings.

Table 1.

All patients were preoperatively evaluated with at least T2-weighted and T1-weighted images. Diffusion-weighted and dynamic contrast-enhanced imaging were optional. MRIs were reviewed by 1 of 3 genitourinary imaging-specialized radiologists (S.H.K., J.Y.C., or S.Y.K.). Definite low signal abnormality on T2-weighted imaging was regarded as a clinically overt disease (Fig. 1). These findings were inte-

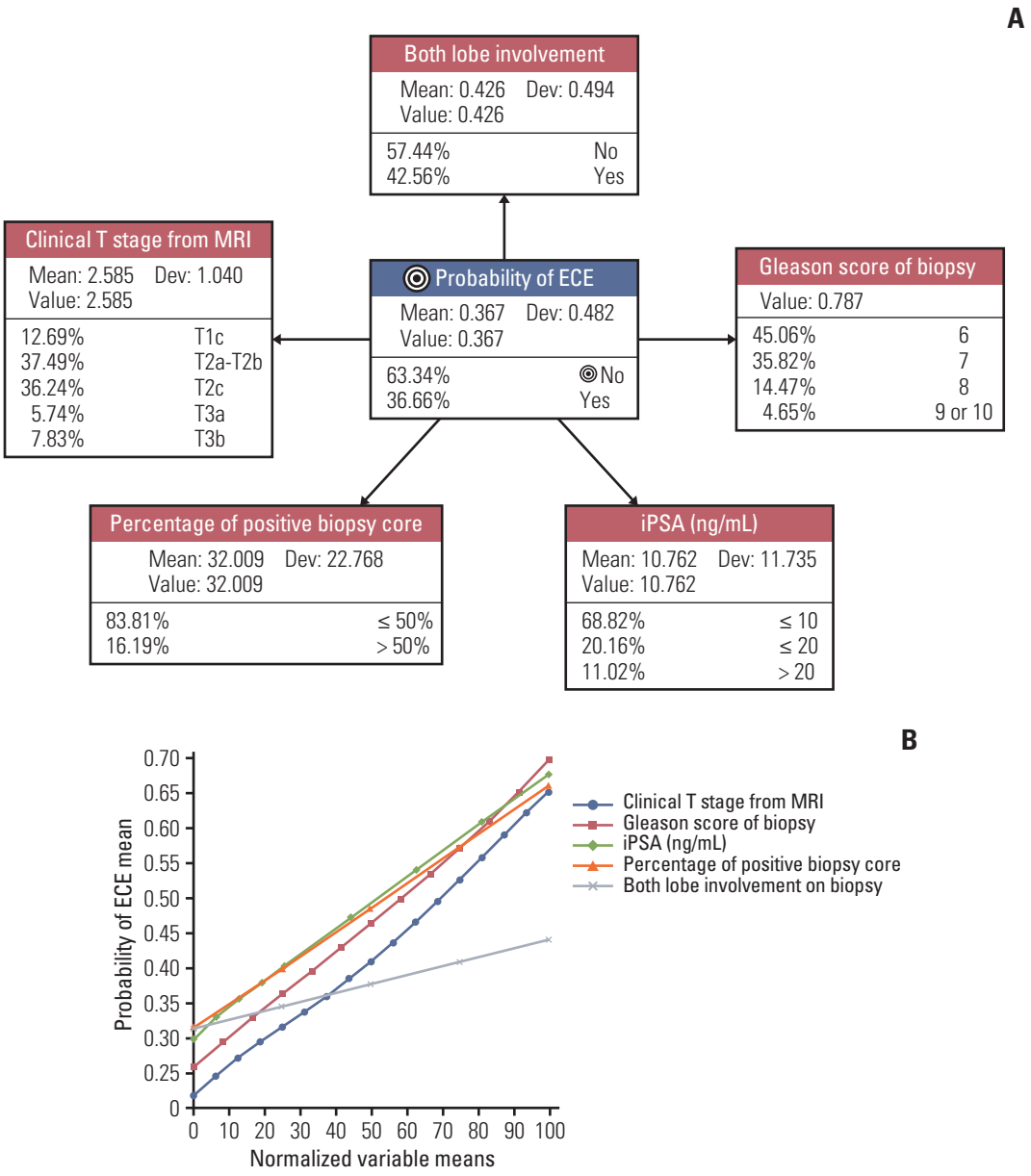

Fig. 2. (A) BN structure to estimate the probability of ECE. Each node demonstrates the associated variable, the discretized state, baseline prevalence, mean, deviation values in the study population. (B) The graph showing the impact of each variable on the probability of ECE. x-axis represents the normalized mean-value of each variable, and y-axis shows the mean probability of ECE. BN, Bayesian network; ECE, extracapsular extension; iPSA, initial prostate-specific antigen; MRI, magnetic resonance imaging.

grated for MRI-based clinical T-staging (cT_{MRI}).

2. Multivariate logistic regression model

Multivariate logistic regression analysis (backward stepwise) was performed using SPSS ver. 22.0 (IBM Corp., Armonk, NY). The iPSA, percentage of positive biopsy cores (PPC), both lobe involvement on biopsy (BLI-Bx), GS, and cT_{MRI} stage were considered as risk factors for predicting ECE, SVI, and RM+ve. All factors were regarded as continuous variables, except BLI on biopsy. GS of 7(4+3) was coded as 7.5 to distinguish from the GS of 7(3+4). The level of statistical significance was set at $p < 0.05$.

3. Establishing and validation of BN models

Three aforementioned pathologic findings were defined as class variables: ECE, SVI, and RM+ve. For each class

Table 3. Performance of BN models

BN models	5-Fold validation metrics		
	Overall AUC[a]	Overall Calibration Index (%)	Overall accuracy (%)
ECE	0.76	79.7	73.0
SVI	0.88	62.6	89.6
RM+ve	0.70	75.1	69.1

AUC, area under the curve; BN, Bayesian network; ECE, extracapsular extension, RM+ve, positive resection margin; SVI, seminal vesicle invasion. [a]Interpretation: 0.5, no discrimination; 0.7-0.8, acceptable; 0.8-0.9, excellent; > 0.9, outstanding [19].

variable, three different BN models were generated [15]. We adopted the naïve Bayes classifier algorithm to establish each BN model and all variables were conditionally independent of the class variable. Therefore, we first selected the variables to be incorporated into the BN model from the multivariate logistic regression model. Afterwards, they were categorized into two to four states. Discretization of continuous variables was applied mostly based on the NCCN risk-grouping system.

For each BN model, we validated the model performance by 5-fold validation. The mean area under the receiver operating characteristic curve (AUC), calibration index, and accuracy were measured. We visualized the impact of each node on the mean value of the class variable while holding the probability distributions of other variables fixed. Additionally, mutual information (MI) was calculated between each node and the class variable to estimate the probabilistic dependence. MI between two random variables X and Y is defined as the difference between the marginal entropy H(X) and its conditional entropy H(X|Y) [16]. H(X) is the entropy for X and H(X|Y) is the conditional entropy for X given Y. MI is intended for measuring the mutual dependence between two random variables. Normalized and relative MIs were computed. In each BN, a clinically interpretable decision tree was generated to estimate the probabilities of risk factors. Finally, each BN model was uploaded to a public Bayesian license server, providing public access to our models. A G-test of independence was performed for MI between two random variables. BN analysis was performed using the BayesiaLab 9.1 (Bayesian Limited Company, France).

4. Internal comparison between the BN model and the Roach formula

The risk of pathological ECE and SVI were calculated in all patients based on the Roach formula as the following: ECE risk (%)=1.5×iPSA+(10×(GS-3)); SVI risk (%)=iPSA+(10×(GS-6)) [17]. Values exceeding 100% were considered as 100%. The DeLong's comparison method was used to compare the performance of BN and Roach models [18].

Table 4. Node significance to the class variable

Node	Normalized mutual information (%)	Relative mutual information (%)	Relative significance	p-value[a]
Node significance to the probability of ECE				
PPC	8.22	8.67	1.000	< 0.001
iPSA (ng/mL)	7.74	8.17	0.942	< 0.001
Gleason scores of biopsy	7.56	7.97	0.920	< 0.001
cT_{MRI} stage[b]	6.63	6.99	0.807	< 0.001
Both lobe involvement	2.62	2.76	0.319	< 0.001
Node significance to the probability of SVI				
cT_{MRI} stage[b]	9.85	18.75	1.000	< 0.001
Gleason scores of biopsy	9.02	17.17	0.916	< 0.001
iPSA (ng/mL)	7.25	13.81	0.736	< 0.001
PPC	7.15	13.61	0.726	< 0.001
Node significance to the probability of RM+ve				
iPSA (ng/mL)	6.40	6.70	1.000	< 0.001
PPC	5.26	5.51	0.822	< 0.001
cT_{MRI} stage[b]	3.76	3.94	0.588	< 0.001
Gleason scores of biopsy	3.57	3.74	0.559	< 0.001

cT_{MRI}, magnetic resonance imaging–based T-staging; ECE, extracapsular extension; iPSA, initial prostate-specific antigen; MRI, magnetic resonance imaging; PPC, percentage of positive biopsy cores; RM+ve, positive resection margin; SVI, seminal vesicle invasion. [a]G-test, [b]Clinical stage according to magnetic resonance imaging findings.

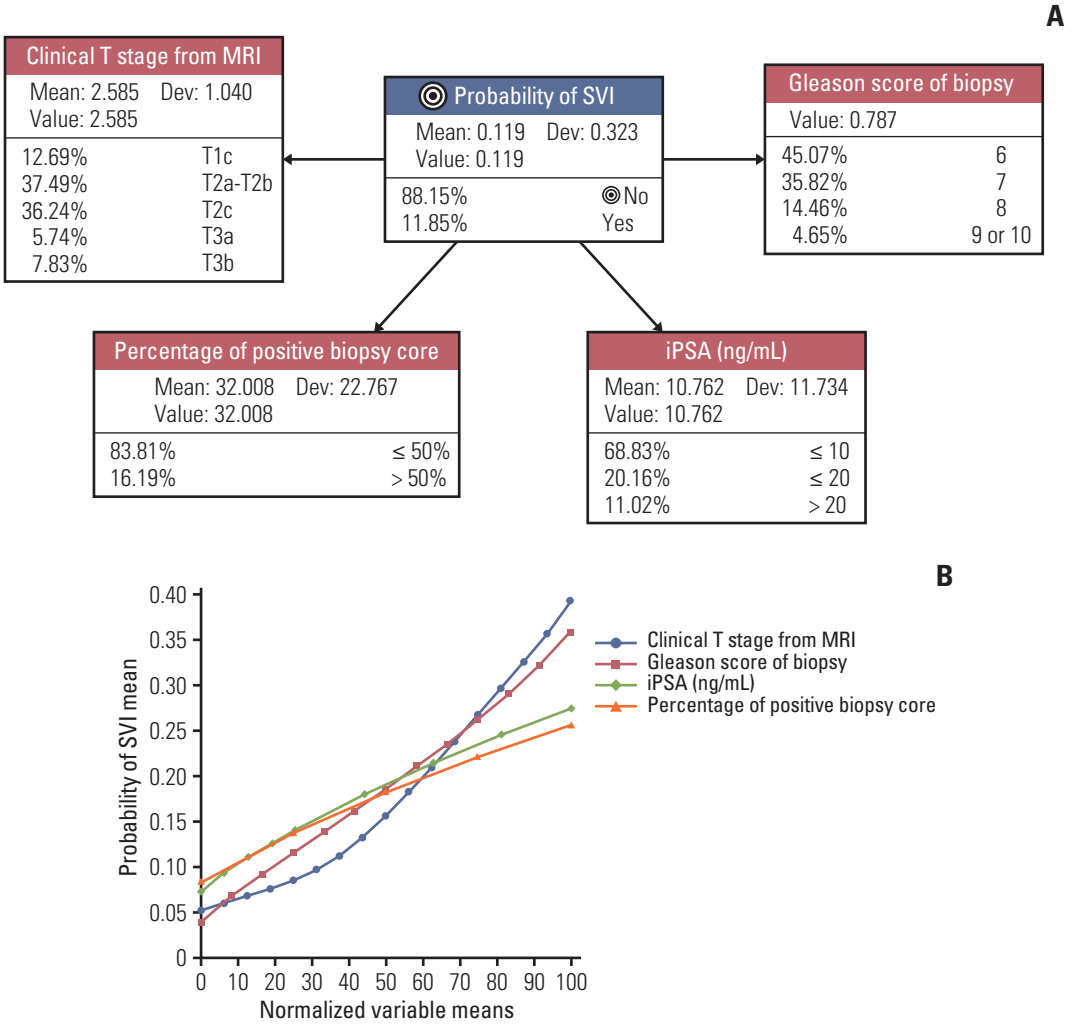

Fig. 3. (A) BN structure to estimate the probability of SVI. Each node demonstrates the associated variable, the discretized state, baseline prevalence, mean, deviation values in study population. (B) The graph showing the impact of each variable on the probability of SVI. x-axis represents the normalized mean-value of each variable, and y-axis shows the mean probability of SVI. BN, Bayesian network; iPSA, initial prostate-specific antigen; MRI, magnetic resonance imaging; SVI, seminal vesicle invasion.

Results

1. Concordance between cT_{MRI} and pathological T-stage

When cT_{MRI} and pathological T-stage were classified in three groups (T1c-T2c, organ-confined; T3a, ECE; T3b, SVI), the concordance rate between cT_{MRI} and pathological T-stage was 66.0% (1,293/1,915). Pathological T-stage was down-staged in only 4.8% (92/1,915). However, up-staging was frequently observed with 29.2% of patients (560/1,915) demonstrating higher pathological T-stage compared to cT_{MRI}. Among 110 patients with cT_{MRI}3a, 14 (12.7%) and 36 (32.7%) patients were up-staged to pT3b and down-staged to pT2, respectively. In 150 patients with cT_{MRI}3b, 32 (21.3%) and 24 (16.0%) patients were down-stage to pT2 and pT3a, respectively.

2. Multivariate logistic regression model

In the multivariate logistic regression model, an increase in iPSA, PPC, GS, and cT_{MRI} were significant risk factors for ECE, SVI, and RM+ve. BLI-Bx was only significant for ECE. Table 2 summarizes the multivariate logistic regression model.

3. Prediction of ECE with BN

The BN structure predicting the probability of ECE is demonstrated in Fig. 2A. Each node of the BN structure had a baseline probability distribution. Five-fold validation revealed that this network had an AUC of 0.76 and an

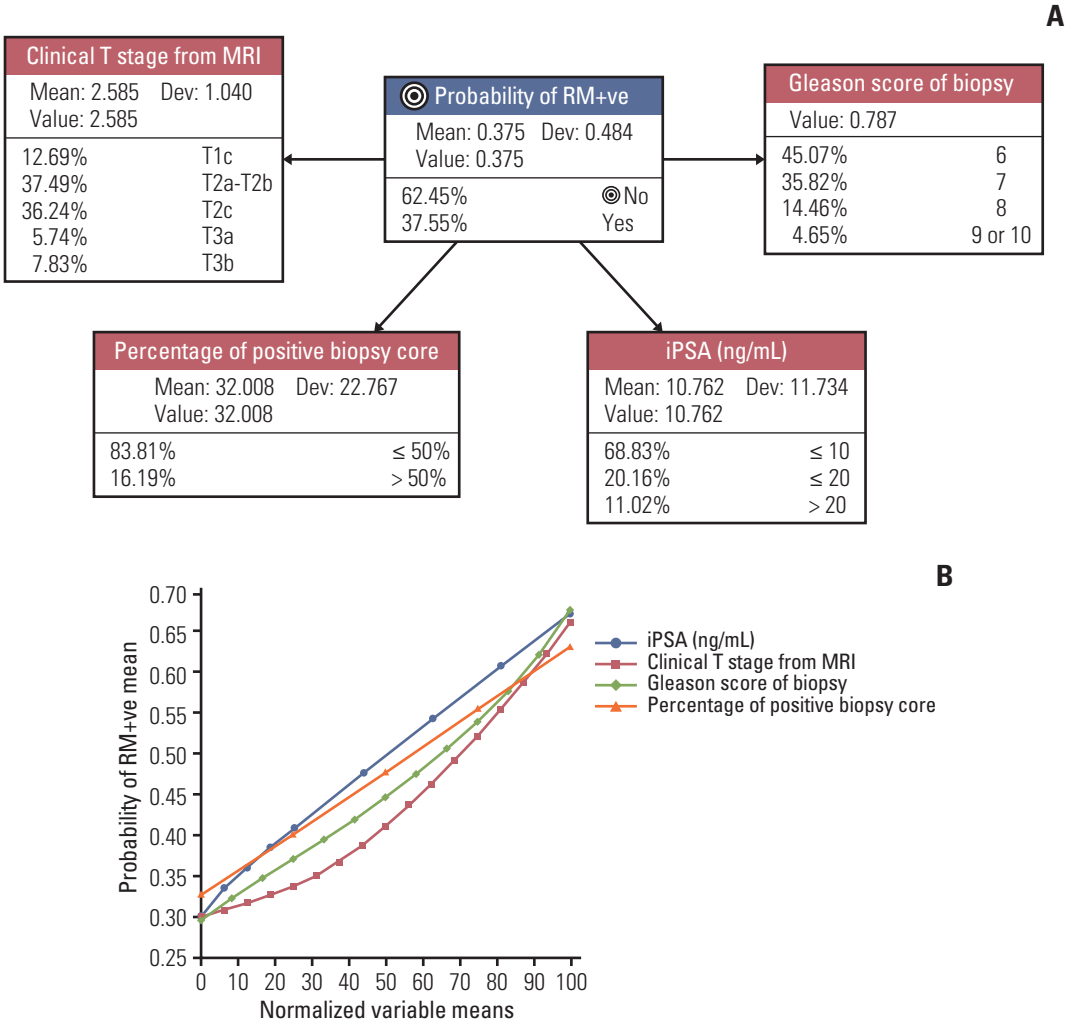

Fig. 4. (A) BN structure to estimate the probability of RM+ve. Each node demonstrates the associated variable, the discretized state, baseline prevalence, mean, deviation values in study population. (B) The graph showing the impact of each variable on the probability of RM+ve. x-axis represents the normalized mean-value of each variable, and y-axis shows the mean probability of RM+ve. BN, Bayesian network; iPSA, initial prostate-specific antigen; MRI, magnetic resonance imaging; RM+ve, positive resection margin.

overall accuracy of 73.0% (Table 3). In addition, the most well-calibrated BN model was the ECE model (calibration index=79.7%). The nodes of the BN model were PPC, iPSA, GS, cT_{MRI}, and BLI-Bx. These nodes all had a linear relationship with the probability of ECE (Fig. 2B). Of these, PPC had a normalized MI of 8.22% (G-test, $p < 0.001$) as the most important factor. On the other hand, BLI-Bx had the lowest normalized MI of 2.62% (G-test, $p < 0.001$) (Table 4). Based on this BN model, the individualized scenarios with the highest risk of ECE are summarized in S1 Fig. It is important to note that the tree does not represent every possible clinical scenario, which can be found in a separate web-user interface.

4. Prediction of SVI with BN

The BN model to predict the probability of SVI included cT_{MRI}, GS, iPSA, and PPC (Fig. 3A). Among the three BN models, SVI prediction model showed the best performance with AUC of 0.88 and overall accuracy of 89.6%. However, its calibration index (62.6%) was the lowest among the BN models (Table 3). The cT_{MRI} and GS of biopsy exponentially increased the probability of SVI (Fig. 3B), with cT_{MRI} being the most important factor for the risk of SVI (normalized MI, 9.85%; $p < 0.001$) (Table 4). Similarly, GS also had significant relative importance (normalized MI, 9.02%; $p < 0.001$). By contrast, both iPSA and PPC showed low relative significance in terms of the risk of SVI. The clinical scenarios with the highest probability of pathological SVI are schematized

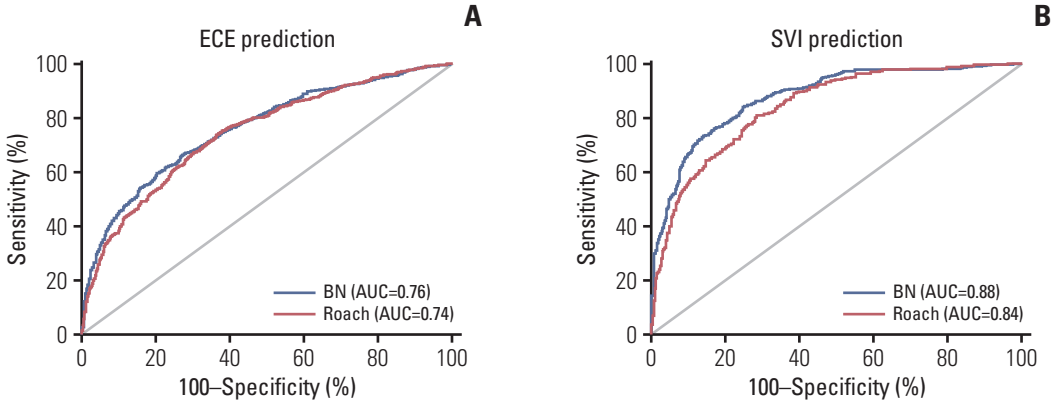

Fig. 5. Comparison between the predictive accuracy of BN model and Roach formula for pathological ECE (A) and SVI (B) according to the DeLong's comparison method. AUC, area under the curve; BN, Bayesian network; ECE, extracapsular extension; SVI, seminal vesicle invasion.

in S2 Fig.

5. Prediction of RM+ve with BN

To predict the probability of RM+ve, we established a BN network model that contained iPSA, PPC, cT_{MRI}, and GS of biopsy (Fig. 4A). The AUC, calibration index, and overall accuracy of this model were 0.70, 75.1%, and 69.1%, respectively (Table 3). The impact of each node on the probability of RM+ve is illustrated in Fig. 3B. Increasing iPSA and PPC were linearly associated with an increased risk of RM+ve. On the other hand, cT_{MRI} and GS exponentially increased the chance of RM+ve (Fig. 4B). The most influential factor was iPSA (normalized MI, 6.40%; $p < 0.001$) followed by PPC (normalized MI, 5.51%, $p < 0.001$) (Table 4). Similar MI and relative importance were observed between cT_{MRI} and GS with regard to the risk of RM+ve. We then generated an interpretation tree of several clinical scenarios with the highest risk of RM+ve (S3 Fig.).

6. Implementation of web-user interface

We implemented each BN model in the web-user interface for convenient use by physicians to estimate the risk of pathological local findings. The web addresses of each model can be found at https://github.com/bigwiz83/SNUHRO_ProstateCancer. Furthermore, individuals accessing the website can test the BN models in private desktop using the uploaded files. An example of the web interface is demonstrated in S4 Fig.

7. AUC values: BN model vs. the Roach formula

In terms of ECE prediction, BN model showed improved performance with marginal significance compared to the Roach formula (AUC, 0.76 vs. 0.74; DeLong's method p=0.060) (Fig. 5A). The BN model for prediction of SVI showed significantly improved performance compared to the Roach model (AUC, 0.88 vs. 0.84; DeLong's method $p < 0.001$) (Fig. 5B).

Discussion

External beam RT with or without brachytherapy or androgen deprivation therapy is a standard treatment option for PCa throughout all risk groups [3,4]. With the routine utilization of intensity-modulated and image-guided RT for PCa, the proportion of PCa patients treated with moderate- to ultra-hypofractionated RT has steeply increased, as supported by biological interpretation of past studies [5]. In this context, precise target delineation can never be emphasized too much.

The current international RT-target delineation guidelines for PCa suggest that ECE and SVI are based on a somewhat simplified risk grouping. The recently published EORTC guidelines suggest adding a 3-mm margin around the prostate for the clinical target volume in order to sufficiently cover possible ECE in intermediate-/high-risk patients [6]. Considering SVI, the guideline recommends including the proximal 1.4-cm and 2.2-cm of the SV in intermediate- and high-risk patients, respectively, when the target is delineated on a planning computed tomography scan [6]. However, there is a small but noted discrepancy in the risk grouping between the EORTC and NCCN guidelines. Clinical T2c disease is regarded as a high-risk factor in the EORTC guidelines, whereas it is an intermediate-risk factor in the NCCN guideline [4,6]. Therefore, it might be more reasonable to individually estimate the probability of ECE or SVI in pati-

ents based on each risk factor that significantly predicts the risk of ECE or SVI and implicate the prediction to RT-target volume delineation. For example, in the PROFIT trial, experimenting with a hypofractionated schedule of 60 Gy in 20 fractions in intermediate-risk PCa, the proximal 1.0-cm SV was included in the clinical target volume only when the predicted risk of SVI exceeded 15% based on Partin's nomogram [20,21]. Similarly, in the CHHiP trial, patients with localized PCa were individualized for inclusion of SV in the clinical target volume based on the findings from Roach [17], not the overall risk grouping [22,23].

Partin's nomogram as well as Roach's formula predict the risk of ECE or SVI with respect to possible individual risk factors, such as clinical T-stage, iPSA, and GS [17,21]. In this context, we developed two separate models using multivariate logistic regression analysis and BN to provide convenient prediction of ECE, SVI, and RM+ve risk to physicians, and to guide RT-target delineation considering all individual factors such as cT_{MRI}, iPSA, GS, PPC, and BLI-Bx. Although pretreatment MRI is an accurate modality when discriminating organ-confined vs. ECE/SVI in PCa [9-11], and those findings are an indicator of relapse or metastases [23,24], MRI is discouraged from being used as a staging modality in the 8th edition of the AJCC staging system [8] as well as in the models from Partin et al. [21] and Roach [17]. Furthermore, detecting SVI with digital rectal exams is prone to error, and the correlation between pathological SVI and clinical staging with digital rectal exam might be poor compared to other risk factors such as iPSA levels, tumor differentiation, or PPC on biopsy [25]. To add the value of MRI in predicting ECE and SVI, we integrated the MRI findings to clinical staging, referred to cT_{MRI} staging in the current study. The cT_{MRI} had the highest correlation with pathological SVI in the BN model (normalized MI, 9.85%; $p < 0.001$). It was also a significant indicator for pathological ECE. The additional value of our models is the integration of PPC, which is also known to increase the risk of ECE, SVI, and RM+ve [25-27]. Indeed, it significantly correlated with all three endpoints in both models (all $p < 0.001$). Due to the wide use of pretreatment MRI, a major portion of radiation oncologists and urologists might already be using the concept of cT_{MRI} in daily practice, although not stipulated in any publication.

A major limitation of using the cT_{MRI} concept is that no standardized criteria for local staging with MRI currently exist, which is a major limitation of our study as well. Although we used a simple criterion of definite low signal intensity on T2-weighted imaging as an abnormal finding, multiparametric MRI (mpMRI) including diffusion-weighted and dynamic contrast-enhanced imaging is the recommended modality currently [3,4,28]. Consecutive efforts are being made to introduce mpMRI findings in clinical practice. For instance, Mehralivand et al. [29] suggested a grading system for extraprostatic extension with mpMRIs based on findings such as the length of contact with the prostatic capsule, capsular bulging, or obliteration of the rectoprostatic angle, which were highly correlated with the presence of actual extraprostatic invasion in their prostatectomy specimen. A report from Giannarini et al. [30] showed that the combination of only two sequences, diffusion-weighted and T2-weighted axial imaging, has comparable performance to mpMRI in predicting pT3 or higher disease. Grivas et al. [31] have also demonstrated a superior accuracy in predicting pathological SVI when mpMRI is added to the Partin model compared to relying on the Partin table alone. It is overt that the more advanced the MRI findings, the higher the risk of pathological ECE, SVI, and RM+ve [9-11]. However, standardization of criterion and quantification of MRI findings in order to be used as a standard staging modality are yet to be done, as well as the integration into the AJCC T-staging of PCa for guiding clinical practice. At this point, cT_{MRI} should be determined mostly by genitourinary expert radiologists.

BN is a probabilistic graphical model for decision support. In the current study, we could infer important associations between variables and class variables such as ECE, SVI, and RM+ve by using BN models. These BN models can practically support risk adapted-treatment of patients because they can instantly respond to the clinician's request or questions with a visual and interpretable representation. In addition, the BN approach can decompose the prediction model and demonstrate how clinical factors affect the predicted class variables. The current study revealed non-linear as well as linear relationships between risk factors, which are not often captured by the logistic regression model. Moreover, MI was calculated to measure the relative importance among variables. The performance of the BN models in the current study were acceptable for predicting ECE and SVI (Table 3), especially SVI. Furthermore, in the internal comparison between the BN model and Roach formula [3], our BN model showed improved AUC values compared to the Roach model for ECE ($p=0.060$) and SVI ($p < 0.001$) prediction, although the difference for ECE was marginally significant and the absolute difference were modest. This might reflect the necessity of integrating MRI findings such as the 'cT_{MRI}' as used in our study to accurately predict pathological findings. However, our BN model warrants external validation in future studies.

In summary, we have successfully developed two models based on the multivariate logistic regression analysis and BN to estimate the risk of pathologic ECE, SVI, and RM+ve based on several clinical factors in PCa. These models are expected to be applied in patients with PCa to predict the risk of pathological ECE, SVI, and RM+ve, and eventually guide radiation oncologists throughout the target-delineat-

ing process and urologists in deciding treatment modality.

Electronic Supplementary Material

Supplementary materials are available at Cancer Research and Treatment website (https://www.e-crt.org).

Ethical Statement

This retrospective study was approved by the Institutional Review Board of the Seoul National University Hospital (IRB No. H-1611-016-805). Informed consent was waived due to the retrospective nature of the study.

Author Contributions

Conceived and designed the analysis: Wee CW, Kim JH.
Collected the data: Wee CW, Jeong CW, Kwak C, Kim HH, Ku JH, Kim SH, Cho JY, Kim SY.
Contributed data or analysis tools: Wee CW, Jang BS, Jeong CW, Kwak C, Kim HH, Ku JH, Kim SH, Kim SY.
Performed the analysis: Wee CW, Jang BS, Kim JH.
Wrote the paper: Wee CW, Jang BS, Kim JH.

Conflicts of Interest

Conflict of interest relevant to this article was not reported.

References

1. Siegel RL, Miller KD, Jemal A. Cancer statistics, 2019. CA Cancer J Clin. 2019;69:7-34.
2. Jung KW, Won YJ, Kong HJ, Lee ES. Cancer statistics in Korea: incidence, mortality, survival, and prevalence in 2016. Cancer Res Treat. 2019;51:417-30.
3. Parker C, Castro E, Fizazi K, Heidenreich A, Ost P, Procopio G, et al. Prostate cancer: ESMO Clinical Practice Guidelines for diagnosis, treatment and follow-up. Ann Oncol. 2020;31:1119-34.
4. NCCN Clinical Practice Guidelines in Oncology. Prostate Cancer, version 2.2020 [Internet]. Plymouth Meeting, PA: National Comprehensive Cancer Network; 2020 [cited 2020 Jul 15]. Available from: https://www.nccn.org/professionals/physician_gls/pdf/prostate.pdf.
5. Morgan SC, Hoffman K, Loblaw DA, Buyyounouski MK, Patton C, Barocas D, et al. Hypofractionated Radiation Therapy for Localized Prostate Cancer: An ASTRO, ASCO, and AUA Evidence-Based Guideline. J Clin Oncol. 2018:JCO1801097.
6. Salembier C, Villeirs G, De Bari B, Hoskin P, Pieters BR, Van Vulpen M, et al. ESTRO ACROP consensus guideline on CT- and MRI-based target volume delineation for primary radiation therapy of localized prostate cancer. Radiother Oncol. 2018;127:49-61.
7. Leyh-Bannurah SR, Dell'Oglio P, Tian Z, Schiffmann J, Shariat SF, Suardi N, et al. A proposal of a new nomogram for predicting upstaging in contemporary D'Amico low-risk prostate cancer patients. World J Urol. 2017;35:189-97.
8. Buyyounouski MK, Choyke PL, McKenney JK, Sartor O, Sandler HM, Amin MB, et al. Prostate cancer: major changes in the American Joint Committee on Cancer eighth edition cancer staging manual. CA Cancer J Clin. 2017;67:245-53.
9. Feng TS, Sharif-Afshar AR, Wu J, Li Q, Luthringer D, Saouaf R, et al. Multiparametric MRI improves accuracy of clinical nomograms for predicting extracapsular extension of prostate cancer. Urology. 2015;86:332-7.
10. Lebacle C, Roudot-Thoraval F, Moktefi A, Bouanane M, De La Taille A, Salomon L. Integration of MRI to clinical nomogram for predicting pathological stage before radical prostatectomy. World J Urol. 2017;35:1409-15.
11. Gupta RT, Brown AF, Silverman RK, Tay KJ, Madden JF, George DJ, et al. Can radiologic staging with multiparametric MRI enhance the accuracy of the partin tables in predicting organ-confined prostate cancer? AJR Am J Roentgenol. 2016;207:87-95.
12. Gevaert O, De Smet F, Timmerman D, Moreau Y, De Moor B. Predicting the prognosis of breast cancer by integrating clinical and microarray data with Bayesian networks. Bioinformatics. 2006;22:e184-90.
13. Cai ZQ, Guo P, Si SB, Geng ZM, Chen C, Cong LL. Analysis of prognostic factors for survival after surgery for gallbladder cancer based on a Bayesian network. Sci Rep. 2017;7:293.
14. Cong LL, Cai ZQ, Guo P, Chen C, Liu DC, Li WZ, et al. Decision of surgical approach for advanced gallbladder adenocarcinoma based on a Bayesian network. J Surg Oncol. 2017;116:1123-31.
15. Husmeier D, Dybowski R, Roberts S. Advanced information and knowledge processing. Probabilistic modelling in bioinformatics. and medical informatics. London: Springer-Verlag; 2005.
16. Yang Y. Information theory, inference, and learning algorithms. J Am Stat Assoc. 2012;100:1461-2.
17. Roach M 3rd. Re: The use of prostate specific antigen, clinical stage and Gleason score to predict pathological stage in men with localized prostate cancer. J Urol. 1993;150:1923-4.
18. DeLong ER, DeLong DM, Clarke-Pearson DL. Comparing the areas under two or more correlated receiver operating characteristic curves: a nonparametric approach. Biometrics. 1988;44:837-45.
19. Hosmer DW Jr, Lemeshow S, Sturdivant RX. Applied logistic regression. 3rd ed. Hoboken, NJ: John Wiley & Sons; 2013.
20. Catton CN, Lukka H, Gu CS, Martin JM, Supiot S, Chung PWM, et al. Randomized trial of a hypofractionated radiation regimen for the treatment of localized prostate cancer. J Clin Oncol. 2017;35:1884-90.
21. Partin AW, Kattan MW, Subong EN, Walsh PC, Wojno KJ, Oesterling JE, et al. Combination of prostate-specific antigen,

clinical stage, and Gleason score to predict pathological stage of localized prostate cancer: a multi-institutional update. JAMA. 1997;277:1445-51.
22. Dearnaley D, Syndikus I, Mossop H, Khoo V, Birtle A, Bloomfield D, et al. Conventional versus hypofractionated high-dose intensity-modulated radiotherapy for prostate cancer: 5-year outcomes of the randomised, non-inferiority, phase 3 CHHiP trial. Lancet Oncol. 2016;17:1047-60.
23. Ahmed HU, Kirkham A, Arya M, Illing R, Freeman A, Allen C, et al. Is it time to consider a role for MRI before prostate biopsy? Nat Rev Clin Oncol. 2009;6:197-206.
24. Muglia VF, Westphalen AC, Wang ZJ, Kurhanewicz J, Carroll PR, Coakley FV. Endorectal MRI of prostate cancer: incremental prognostic importance of gross locally advanced disease. AJR Am J Roentgenol. 2011;197:1369-74.
25. Tsurumaki Y, Tomita K, Kume H, Yamaguchi T, Morikawa T, Takahashi S, et al. Predictors of seminal vesicle invasion before radical prostatectomy. Int J Urol. 2006;13:1501-8.
26. Guzzo TJ, Vira M, Wang Y, Tomaszewski J, D'Amico A, Wein AJ, et al. Preoperative parameters, including percent positive biopsy, in predicting seminal vesicle involvement in patients with prostate cancer. J Urol. 2006;175:518-21.
27. Lieberfarb ME, Schultz D, Whittington R, Malkowicz B, Tomaszewski JE, Weinstein M, et al. Using PSA, biopsy Gleason score, clinical stage, and the percentage of positive biopsies to identify optimal candidates for prostate-only radiation therapy. Int J Radiat Oncol Biol Phys. 2002;53:898-903.
28. Murphy G, Haider M, Ghai S, Sreeharsha B. The expanding role of MRI in prostate cancer. AJR Am J Roentgenol. 2013;201:1229-38.
29. Mehralivand S, Shih JH, Harmon S, Smith C, Bloom J, Czarniecki M, et al. A grading system for the assessment of risk of extraprostatic extension of prostate cancer at multiparametric MRI. Radiology. 2019;290:709-19.
30. Giannarini G, Cereser L, Como G, Bonato F, Pizzolitto S, Valotto C, et al. Accuracy of abbreviated multiparametric MRI-derived protocols in predicting local staging of prostate cancer in men undergoing radical prostatectomy. Acta Radiol. 2021;62:949-58.
31. Grivas N, Hinnen K, de Jong J, Heemsbergen W, Moonen L, Witteveen T, et al. Seminal vesicle invasion on multi-parametric magnetic resonance imaging: correlation with histopathology. Eur J Radiol. 2018;98:107-12.